Japanese Journal of Applied Physics
Vol. 46, No. 4A, 2007, pp. 1680–1691

Numerical Study of Neutral Gas Transport in Linear Plasma Device

Maxim IGNATENKO*, Masafumi AZUMI[1], Masatoshi YAGI, Shunjiro SHINOHARA[2], Sanae-I ITOH, and Kimitaka ITOH[3]

Research Institute of Applied Mechanics, Kyushu University, Kasuga, Fukuoka 816-8580, Japan
[1]*Center of Computational Science and Engineering, Japan Atomic Energy Agency, Tokyo 110-0015, Japan*
[2]*Interdisciplinary Graduate School of Engineering Sciences, Kyushu University, Kasuga, Fukuoka 816-8580, Japan*
[3]*National Institute for Fusion Science, Toki, Gifu 509-5292, Japan*

(Received October 13, 2006; accepted January 10, 2007; published online April 5, 2007)

Possible methods of controlling the neutral gas pressure in a linear plasma device are numerically investigated. For this purpose, the neutral gas transport in argon plasma is calculated by means of Monte Carlo method. The code takes into account the self-elastic collisions along with the elastic neutral–ion and the electron impact ionization collisions. The effects of a baffle plate, the electron temperature, the pump speed, and plasma flow on the neutral density are evaluated within a range of experimental conditions. The baffle plate is found to affect the amount of neutral gas when the electron temperature is low and the plate is located close to a neutral source. As the electron temperature increases, electron ionization strongly enhances the recycling of neutral gas, thus making the role of the baffle plate weaker. It is clarified that the electron ionization is a key factor of the neutral transport in a linear plasma device with low density and low electron temperature.
[DOI: 10.1143/JJAP.46.1680]

KEYWORDS: simulation, Monte Carlo, neutral transport, baffle plate

1. Introduction

It is well known that the unique structure of non equilibrium plasma is self-generated through nonlinear interactions among the plasma instabilities. Since the fluctuations induce various complex aspects in the plasmas, the understanding of the physics of turbulence is considered to be one of the most important research targets in plasma physics and controlled fusion. For example, recently special attention has been paid to the formation of the zonal flow as a means of studying the key physical concepts in turbulence.[1)] So far, basic experiments have been performed to study the basic features of plasma turbulence in several linear devices.[2–7)]

With this background, a systematic study on turbulent plasma dynamics has been undertaken by combining theory, numerical simulation using a "Numerical Linear Device" (NLD) code,[8)] and experiments using a straight mirror device "Large Mirror Device" (LMD).[9–11)] The aim of the experiment is to excite drift-wave instabilities to study the turbulent state of plasma. Preliminary theoretical studies and numerical simulation suggest that collisions of ions with neutrals may play an important role in the resistive drift-wave instabilities, and give a threshold condition for the turbulence excitation.[12)] Therefore, the neutral pressure should be reduced to as low as possible in experiments using a LMD. On the other hand, since a neutral gas of finite pressure is necessary for plasma production, a suitable neutral pressure in the production region should be maintained. In a LMD, the separation between the plasma production region and the confinement region is not complete, and the neutral pressure is high in the whole region of the discharge tube. Therefore, the neutral pressure should be controlled. Assuming the neutral temperature to be constant, the neutral pressure profile corresponds to that of the neutral density.

In this paper, possible methods of controlling the number of neutrals in a LMD are investigated by numerical evaluation of the Boltzmann equation for various atomic processes. The Monte Carlo method is utilized to calculate the neutral density profiles based on experimentally measured plasma parameters. If the neutral pressure in the device is sufficiently high (mTorr range) and the effective ionization ratio is low, self-elastic collisions are considered to play an important role in determining the neutral pressure profile. They introduce a nonlinear term in the Boltzmann equation, and the solution is obtained by means of an iteration scheme. Furthermore, other atomic processes such as elastic neutral–ion collisions and electron impact ionization collisions are also taken into account.

In the simulation, the system is considered to be two-dimensional, since a LMD consists of a plasma production tube and a cylindrical main chamber connected in series. Although some equipments like vacuum pumps break the axisymmetry, their ports are small and the profile in the axial direction is of primary importance in studying neutral transport. In addition, the plasma is assumed to be uniform in the axial direction. In future, the simulation model will be upgraded to include the two-dimensional plasma profiles.

Three neutral sources are considered: gas injection, and plasma recombination on the end plate and in plasma. The particles are exhausted from the device due to ionization or the use of vacuum pumps. The selection of the pump positions and speed is the target of the simulation. In addition to the pumps, a baffle can be installed, which is utilized to isolate injected particles or the end-plate source from the main plasma region. In the former case, the plate is expected to facilitate the accumulation of neutrals in the production tube. In the latter case, it redirects the neutrals to the pump locations. In the paper, the region of applicability of the baffles is quantitatively outlined. The end-plate-side baffle is shown to decrease the neutral level if the electron temperature is relatively low and the speed of the plasma flow exceeds some critical value. Otherwise, the baffle increases the neutral level. If the temperature is high, the neutral profile inside the plasma is strongly damped by the electron impact ionization. Outside the plasma, the neutral profile is mainly determined by the influx and the pumping

*E-mail address: maxim@riam.kyushu-u.ac.jp

speed. A fast pump efficiently reduces the neutral level within the whole experimental device including the production tube. Therefore, the use of an injection-side baffle is suggested to maintain a high neutral level inside the production region. The results discussed in this article are implemented in the design of a "Large Mirror Device-Upgrade" LMD-U.[10)]

In this paper, the basic equations and the numerical scheme are described in detail in §2. The numerical results are presented in §3, where the effects of the baffle plate and the electron temperature are investigated. Finally, the main results are summarized in §4.

2. Numerical Scheme

2.1 Governing equations

In steady state, the statistical distribution of the neutral particles $f_n(\mathbf{r}, \mathbf{v})$ is described by the Boltzmann equation:

$$\mathbf{v}\frac{\partial f_n}{\partial \mathbf{r}} = C(f_n) + S, \tag{2.1}$$

where $\mathbf{v}$ is the particle velocity, $C(f_n)$ is the collision term, and S is the source term. For the present calculation, balance between the distributions of incident $f_{n,inc}$ and reflected $f_{n,rfl}$ particles is fulfilled at the boundary:[13)]

$$f_{n,rfl}|_{\mathbf{r}=\mathbf{r}_{bnd}} = [R_s f_{n,inc}(v_\perp \to -v_\perp) + R_d \Gamma_{inc} F_d]|_{\mathbf{r}=\mathbf{r}_{bnd}}. \tag{2.2}$$

Here, the vector $\mathbf{r}_{bnd}$ points to the boundary (chamber walls, baffle plate, end plate, source positions, or pump ducts), $v_\perp$ is the component of the incident particle velocity toward the boundary, R_s and R_d are the coefficients of specular and diffusive reflection, respectively, $\Gamma_{inc} = \int \mathbf{v}_\perp f_n(v_\perp > 0) d\mathbf{v}$ is the flux of the neutrals towards the wall, and the distribution of the diffusively emitted particles F_d is normalized by $\int_0^\infty v_\perp F_d \, d\mathbf{v} = 1$. At the pump duct position, the specular reflection coefficient R_s is replaced by $1 - \gamma$, where γ is the pump efficiency. In the general case, all parameters on the right-hand side are functions of the particle velocities and positions.

In contrast to the conventional calculations of fusion plasmas, in the case of the simulated linear device, the neutral self-collisions $C_n(f_n, f_n)$ are expected to play an important role due to the high neutral density, making the Boltzmann equation nonlinear. As well as the self-collisions, electron impact ionization $C_e(f_n, f_e)$ significantly affects the neutral profiles. To take into account the energy transport from ions to neutral particles, the elastic ion–neutral collisions $C_i(f_n, f_i)$ are also considered:

$$C(f_n) = C_n(f_n, f_n) + C_i(f_n, f_i) + C_e(f_n, f_e), \tag{2.3}$$

with

$$C_n(f_n, f_n) = \iint I_{els}(u, \mathbf{\Omega}) u (f_n' f_n' - f_n f_n) \, d^3 v_2 \, d\mathbf{\Omega}, \tag{2.4}$$

$$C_i(f_n, f_i) = \iint I_{mom}(u, \mathbf{\Omega}) u (f_n' f_i' - f_n f_i) \, d^3 v_2 \, d\mathbf{\Omega} + \iint I_{cxr}(u, \mathbf{\Omega}) u (f_n' f_i' - f_n f_i) \, d^3 v_2 \, d\mathbf{\Omega}, \tag{2.5}$$

$$C_e(f_n, f_e) = -\iint I_{ion}(u, \mathbf{\Omega}) u \, f_n f_e \, d^3 v_2 \, d\mathbf{\Omega}, \tag{2.6}$$

where I_{els}, I_{mom}, I_{cxr}, and I_{ion} are the self-elastic, ion momentum transfer, resonance charge exchange, and electron impact ionization differential cross sections, respectively, f_e and f_i are the electron and ion distribution functions, respectively, $u = |\mathbf{v}_1 - \mathbf{v}_2|$, $\mathbf{v}_1$ and $\mathbf{v}_2$ are the incident and the target particle velocities, respectively, and $\mathbf{\Omega}$ is the scattering solid angle. The distribution functions of the scattered particles are marked by primes.[14)]

The linear collision terms C_i and C_e can be reduced to simplified forms by assuming isotropic scattering: $I(u, \Omega) = I(u)$. In this case, integration over the solid angle Ω is performed explicitly, and the differential cross sections $I(u)$ are replaced by the corresponding total cross sections $\sigma(u) = \int I(u) \, d\mathbf{\Omega} = 4\pi I(u)$. Next, note that the electron speed $|\mathbf{v}_e|$ is clearly much larger than that of neutrals $|\mathbf{v}_n|$. Therefore, in the case of impact ionization, the relative speed is given by $u \approx |\mathbf{v}_e|$ and the ionization collision term reduces to

$$C_e(f_n, f_e) = -n_e \langle \sigma_{ion} u \rangle f_n, \tag{2.7}$$

where $\langle \sigma_{ion} u \rangle = \int |\mathbf{v}_e| \sigma_{ion}(|\mathbf{v}_e|) F_e(\mathbf{v}_e) \, d^3 v_e$ is the ionization rate coefficient, and the distribution function f_e is assumed to be product of the electron density n_e and the electron velocity distribution F_e.

In the case of the ion collision term, the products $\sigma_{mom}(u)u$ and $\sigma_{cxr}(u)u$ are slowly varying functions of the relative velocity in the region of interest, and thus they can be placed outside the integrands:[13,15)]

$$C_i(f_n, f_i) = n_i(\langle \sigma_{mom}(u)u \rangle + \langle \sigma_{cxr}(u)u \rangle) \times \left[F_i(\mathbf{v} - \mathbf{V}_i) \int f_n(\mathbf{v}') \, d^3 v' - f_n(\mathbf{v}) \right], \tag{2.8}$$

where $f_i = n_i F_i$, with n_i being the ion density and F_i being the ion velocity distribution; the mean ion velocity $\mathbf{V}_i$ is shown explicitly.

In contrast to the linear collision integrals, eqs. (2.5) and (2.6), the neutral self-collision term cannot be easily simplified because of its nonlinear nature. In this article, a stationary state is searched for, and the nonlinear operator $C_n(f_n, f_n)$ is treated by iterations:

$$\mathbf{v}\frac{\partial f_{n,k+1}}{\partial \mathbf{r}} = C_n(f_{n,k+1}, f_{n,k}) + C_i(f_{n,k+1}, f_i) + C_e(f_{n,k+1}, f_n) + S_{k+1}, \tag{2.9}$$

where k is the iteration number. In this case, the C_n term in each iteration step is calculated using the distribution of the previous step distribution and thus it becomes linear. Therefore, within each iteration step it can be written in a similar form to eq. (2.8):

$$C_n(f_{n,k+1}, f_{n,k}) = n_{n,k} \langle \sigma_{els}(u)u \rangle \times \left[F_{n,k}(\mathbf{v} - \mathbf{V}_n) \int f_{n,k+1}(\mathbf{v}') \, d^3 v' - f_{n,k+1}(\mathbf{v}) \right], \tag{2.10}$$

where $f_{n,k} = n_{n,k} F_{n,k}$, and $n_{n,k}$ and $F_{n,k}$ are the neutral density and velocity distribution obtained from the previous iteration step respectively, and $\mathbf{V}_n$ is the neutral mean velocity.

In the iteration scheme, the zero order test function $f_{n,0} = n_{n,0} F_{n,0}$ can be chosen arbitrarily. In the present simulation, the zero-order neutral profile $n_{n,0}$ is taken to be uniform, $n_{n,0} = \int_{inj} \Gamma_{inj} \, d^2 r / P$ and the velocity distribution is $F_{n,0} = \delta(v - v_{th})$, where Γ_{inj} is the injected particle flux, P is the pump speed, $v_{th} = \sqrt{2k_B T_n / M_n}$ is the most probable speed of neutrals, k_B is Boltzmann's constant, T_n is the neutral temperature, and M_n is the mass of a neutral particle. Here,

the zero-order mean velocity is assumed to be zero. Rigorously speaking, the final converged solution ($k \to \infty$) may depend on the choice of the initial conditions at $k = 0$. Such critical dependence on the initial conditions was not found.

To complete the definition of the problem, the source term S has to be explained. The neutral particles are assumed to originate from gas injection S_{inj} and the recombination of ions at the end plate S_{ep} and in the plasma S_{pl}:

$$S = S_{\mathrm{inj}} + S_{\mathrm{ep}} + S_{\mathrm{pl}}, \tag{2.11}$$

where S_{inj} is the prescribed term describing the injected particles, and S_{ep} can be obtained from the distribution of charge particles and the properties of the end plate. To determine S_{pl}, a steady-state condition is used. Namely, the ionization rate is equal to the recombination rate:

$$\iint C_{\mathrm{e}}\, d^3v\, d^3r = \iint S_{\mathrm{ep}}\, d^3v\, d^3r + \iint S_{\mathrm{pl}}\, d^3v\, d^3r, \tag{2.12}$$

where the integrals are calculated over the plasma volume.

The first term on the right-hand side of eq. (2.12) is the number of neutral particles originating on the end plate per second due to the recombination of ions on the end plate:

$$J_{\mathrm{ep}} = \int_{\mathrm{ep}} n_{\mathrm{i}} V_{\mathrm{i}\perp}\, d^2r, \tag{2.13}$$

where $n_{\mathrm{i}} V_{\mathrm{i}\perp} = \Gamma_{\mathrm{i,ep}}$ is the ion particle flux at the end plate, and the plasma flow is assumed to be formed by the ion drift only. The integral is evaluated over the end plate surface. All ions at the end plate are assumed to be neutralized i.e., $\iint S_{\mathrm{ep}}\, d^3v\, d^3r \equiv \Gamma_{\mathrm{n,ep}} = \Gamma_{\mathrm{i,ep}}$.

Finally, from eqs. (2.12) and (2.13) the number of particles originating in the plasma due to recombination J_{pl} is

$$J_{\mathrm{pl}} = \iint C_{\mathrm{e}}\, d^3v\, d^3r - \int_{\mathrm{ep}} n_{\mathrm{i}} V_{\mathrm{i}\perp}\, d^2r. \tag{2.14}$$

The latter expression does not provide information regarding the position of the originated particles. In the present, for the sake of simplicity, recombination inside the plasma is replaced by that at the radial plasma boundary, and is distributed uniformly in the axial and azimuthal directions.

The direction and speed of the new particles can be chosen on the basis of physical reasons or assumptions. In the present version of the code, all source particles have a speed of v_{th} and are directed randomly.

2.2 *Monte Carlo method*

To obtain the neutral gas density distribution in the linear device, the Boltzmann equation [eq. (2.1)] is numerically evaluated by the Monte Carlo method. A general discussion of the method and the application of the algorithm to the neutral profile calculations can be found elsewhere.[15–19] Here, only a brief outline of the method is presented.

During the simulation, N_{src} test flights with an initial dimensionless weight of $w = 1$ are generated for each source. Here, the subscript "src" is given to terms regarding the injected neutrals ("inj") and particles recombining on the end plate ("ep") or in the plasma ("pl"). If the source produces J_{src} particle/s, then each flight is represented by $J_{\mathrm{src}}/N_{\mathrm{src}}$ particle/s at its start.

For the present calculation, the number of injected particles J_{inj} is a prescribed value, determined by the conditions of the experiment. The number of particles originating at the end plate J_{ep} is given by eq. (2.13) and that of particles originating at the plasma surface J_{pl} is defined by eq. (2.14), which is transformed into

$$J_{\mathrm{pl}} = \frac{\kappa_{\mathrm{inj,ion}} J_{\mathrm{inj}} - (1 - \kappa_{\mathrm{ep,ion}}) J_{\mathrm{ep}}}{1 - \kappa_{\mathrm{pl,ion}}}, \tag{2.15}$$

where $\kappa_{\mathrm{src,ion}} = \sum_j w_{(\mathrm{src,ion}),j}/N_{\mathrm{src}}$ is the fraction of ionized particles for each source type, $w_{(\mathrm{src,ion}),j}$ is the weight of the ionized particle and a summation is taken over all ionized particles. The sign of J_{pl} can be used as a test parameter; a negative J_{pl} indicates that the input parameters are incorrect.

Each flight follows its trajectory with a prescribed short step dl. At each step, collision events are tested one after another.

(1) First, the elastic self-collision event is checked: if $\mathrm{rnd}_1 < dl/\lambda_{\mathrm{els}}$ holds, then the event has occurred and a new direction of propagation is randomly chosen. Here, rnd_1 is a uniformly distributed random number (URN), $\lambda_{\mathrm{els}} = 1/(\sqrt{2} n_{\mathrm{n}} \sigma_{\mathrm{elas}})$ is the self-collision mean free path (MFP), $\sqrt{2}$ takes the relative motion of the neutrals into account.

(2) Next, if $\mathrm{rnd}_2 < dl/\lambda_{\mathrm{mom}}$ holds, where rnd_2 is a URN and $\lambda_{\mathrm{mom}} = v_{\mathrm{n}}/[\bar{u}_{\mathrm{i}} n_{\mathrm{i}} (\sigma_{\mathrm{mom}} + \sigma_{\mathrm{chr}})]$ is the ion–neutral collision MFP (v_{n} is the speed of the test particle and $\bar{u}_{\mathrm{i}}$ is the average ion speed), then an ion elastic collision has occurred. In this case, the speed of the flight becomes equal to $\mathbf{V}_{\mathrm{i,drift}}$ and a new direction is randomly chosen.

(3) Finally, if $\mathrm{rnd}_3 < dl/\lambda_{\mathrm{ion}}$, where rnd_3 is a URN and $\lambda_{\mathrm{ion}} = v_{\mathrm{n}}/(n_{\mathrm{e}} \langle \sigma_{\mathrm{ion}} u \rangle)$ is the ionization MFP, then a ionization event has occurred and $w = 0$.

(4) If there is no collision, then the flight makes the next step in the previous direction.

All events are put in order of importance. The self-elastic collision changes the direction of the flight but does not change the particle energy and weight, and it is tested first. The ion-elastic collision affects the particle speed but does not change the particle weight. The ionization can significantly affect the neutral profile, and therefore it is checked last. The proposed scheme allows us to accurately examine the ionization rate, even if the neutral density is high and the step dl is comparable to the total MFP.

The exhaust by the vacuum pump is simulated by reducing the weight of the test flight that hits the pump duct area:

$$w_{\mathrm{rfl}} = \begin{cases} w_{\mathrm{inc}}(1 - P/(S_{\mathrm{pmp}} v_\perp)), & P/(S_{\mathrm{pmp}} v_\perp) < 1, \\ 0, & P/(S_{\mathrm{pmp}} v_\perp) \geq 1, \end{cases} \tag{2.16}$$

where w_{rfl} and w_{inc} are the weights of the flight after and before hitting the pump, P is the pump speed, S_{pmp} is the pump duct area and $v_\perp$ is the component of the flight velocity normal to the pump duct surface.

The flight is traced until its weight becomes smaller than a prescribed threshold.

The calculation domain is divided into cells, and at each flight step various data are accumulated at the corresponding cell. At the end of each iteration, the accumulated data

are transformed into physical quantities. For example, the average neutral density can be obtained as

$$\bar{n}_{\mathrm{n}}(l) = \frac{dl}{V(l)} \sum_{\mathrm{src}} \frac{J_{\mathrm{src}}}{N_{\mathrm{src}}} \sum_{\mathrm{flights}} \frac{w(l)}{|\mathbf{v}_{\mathrm{n}}(l)|}, \tag{2.17}$$

where l is the number of the cell, $\mathbf{v}_{\mathrm{n}}(l)$ is the velocity of the test flight at the cell location, V is the volume of the cell, and summation is taken over all flights passing through the cell. Similarly, the average component or absolute value of the neutral velocity is

$$\bar{v}_{\mathrm{n},j}(l) = \frac{dl}{\bar{n}_{\mathrm{n}}(l)V(l)} \sum_{\mathrm{src}} \frac{J_{\mathrm{src}}}{N_{\mathrm{src}}} \sum_{\mathrm{flights}} \frac{w(l)v_{\mathrm{n},j}(l)}{|\mathbf{v}_{\mathrm{n}}(l)|}. \tag{2.18}$$

Here, $v_{\mathrm{n},j}$ is the component or absolute value of the test flight velocity at the cell location.

2.3 Validation of the model

First, the iteration algorithm is validated. For this, diffusion of the neutral gas in a cylindrical tube without plasma is considered. The length of the tube is L and the radius is r_{tube}. At the rear side of the tube, a semipermeable membrane with reflection coefficient R is located. Every second, J_{inj} particles are injected in the tube uniformly. The front and radial walls are assumed to be absolute reflectors; hence, the particles can only leave the tube through the membrane.

An analytical expression for the neutral density can be obtained from the steady-state one-dimensional continuity equation:

$$\frac{d\Gamma}{dz} = 0, \tag{2.19}$$

where Γ is the total particle flux. A neutral gas with a high density is considered, such that the MFP of a collision is much shorter than the system characteristic size. The semipermeable membrane is assumed to cause a constant gas stream. In this case, the flux is related to the diffusion and streaming terms:

$$\Gamma = \Gamma_0 + D\frac{dn_{\mathrm{n}}}{dz}, \tag{2.20}$$

where Γ_0 is the constant stream flux, $D = \bar{v}_{\mathrm{n}}/(3\sqrt{2}n_{\mathrm{n}}\sigma_{\mathrm{els}})$ is the diffusion coefficient, and $\bar{v}_{\mathrm{n}} = \sqrt{8k_{\mathrm{B}}T_{\mathrm{n}}/(\pi M_{\mathrm{n}})}$ is the average speed of propagation of the neutrals. Therefore, from eqs. (2.19) and (2.20), the shape of the profile is determined as

$$n_{\mathrm{n}}(z) = n_{\mathrm{n}}(0)\mathrm{e}^{-z/\lambda_{\mathrm{eff}}}, \tag{2.21}$$

where λ_{eff} is the effective MFP, which must be determined from boundary conditions, together with $n_{\mathrm{n}}(0)$.

Indeed, at the boundary, the particle fluxes are defined. From the steady-state condition, the total flux through any tube section is constant and is equal to the influx. Therefore,

$$\Gamma|_{z=0} = \Gamma_{\mathrm{inj}}, \tag{2.22}$$

where $\Gamma_{\mathrm{inj}} = J_{\mathrm{inj}}/(\pi r_{\mathrm{tube}}^2)$.

At the membrane position, the fluxes of the reflected and the incident particles are related to each other through the reflection coefficient, giving a total flux of[20)]

$$\Gamma|_{z=L} = \frac{n_{\mathrm{n}}\bar{v}_{\mathrm{n}}}{2}\frac{1-R}{1+R}. \tag{2.23}$$

Equations (2.20)–(2.23) allow us to obtain the neutral density depending on the parameter Γ_0. For the sake of the model validation, the definition of the particle flux through the mean flow speed of particles is more conveniently given as

$$\Gamma = n_{\mathrm{n}}V_{\mathrm{d}}. \tag{2.24}$$

In this case, at the boundaries:

$$n_{\mathrm{n}}V_{\mathrm{d}}|_{z=0} = \Gamma_{\mathrm{inj}}, \tag{2.25}$$

$$V_{\mathrm{d}}|_{z=L} = \frac{\bar{v}_{\mathrm{n}}}{2}\frac{1-R}{1+R}, \tag{2.26}$$

$$n_{\mathrm{n}}|_{z=L} = \frac{2\Gamma_{\mathrm{inj}}}{\bar{v}_{\mathrm{n}}}\frac{1+R}{1-R}. \tag{2.27}$$

Equations (2.21), and (2.25)–(2.27) form the analytical statement of the problem and can be easily solved. The statement is not a closed one, since the boundary conditions depend on the flow speed V_{d}, which was not determined. Therefore, the solution has a unknown parameter,

$$n_{\mathrm{n}} = \frac{\Gamma_{\mathrm{inj}}}{V_{\mathrm{d}}|_{z=0}}\left(\frac{V_{\mathrm{d}}|_{z=0}}{V_{\mathrm{d}}|_{z=L}}\right)^{z/L}. \tag{2.28}$$

Here, $V_{\mathrm{d}}|_{z=L}$ is determined by eq. (2.26) and $V_{\mathrm{d}}|_{z=0}$ is the parameter. Nevertheless, the analytically obtained solution can be compared with the numerical one. First of all, at the exhaust port, the flow speed and neutral density depend on the input parameters only, and thus they can be directly compared with the results of simulation. Then, from the numerical calculations, it is possible to determine the parameter $V_{\mathrm{d}}|_{z=0}$, and therefore the shapes of the analytical and numerical solutions can be also compared, as shown in Fig. 1. Here, arrows indicate the neutral density obtained using eq. (2.27). Symbols show the radially averaged numerical neutral profiles, and lines show the analytical solutions obtained from the mean speed of the particles in the simulation.

During the simulation, to ensure that λ_{elas} is much smaller than the dimensions of the tube, the number of injected particles was chosen to be $J_{\mathrm{inj}} = 2.0 \times 10^{21}$ particle/s, with tube length $L = 2\,\mathrm{m}$ and radius $r_{\mathrm{tube}} = 0.5\,\mathrm{m}$. The results demonstrate that the numerical algorithm is able to accurately calculate the shape and value of the profile for a wide range of reflection coefficients. The relative error between the analytical and numerical solutions in the main region is within 5% [Fig. 1(b)]. Only close to the boundaries the error is large, since the solution [eq. (2.28)] is not valid here due to the lack of interparticle collisions.

3. Simulation Results

3.1 Parameters of simulation

The neutral gas transport in LMD[9,11)] and LMD-U[10)] experimental devices is calculated. Both devices consist of a plasma production tube and a main chamber. A schematic view of the devices is shown in Fig. 2. In the production tube, the neutral gas is injected from the port at the end of the tube and it is ionized by a helicon source. The plasma flows into the main chamber and is terminated at the end plate. The neutral gas is removed by vacuum pumps in the

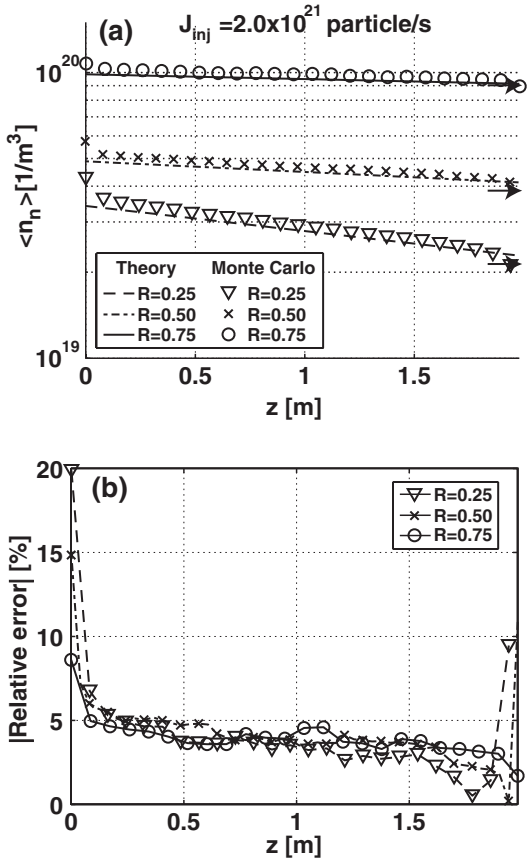

Fig. 1. (a) Radially averaged numerical (symbols) and analytical neutral profiles (lines) $\langle n_n \rangle$ and (b) relative error of calculation. The number of the injected particles is $J_{inj} = 2.0 \times 10^{21}$ particle/s, $L = 2$ m, and $r_{tube} = 0.5$ m. Arrows indicate values obtained using eq. (2.27).

main chamber. For the single pump case, the pump is set near the end plate. Baffle plates with a radius of 0.06 m can be installed in the main chamber to control the neutral gas pressure. The device is assumed to be axisymmetric. The parameters of LMD and LMD-U used in the following calculations are summarized in Table I.

In the case of the LMD, the length of the chamber is 1.7 m. The number of the injected particles is set to $J_{inj} = 1.28 \times 10^{19}$ particle/s and the pump speed is 400 L/s, such that the gas pressure, which is defined as the ratio of J_{inj} to the pump speed, is 1 mTorr at room temperature. The maximum magnitude of the magnetic field is 0.12 T. In the simulation, to study the effect of the baffle plate, the pump position is shifted from its real position toward the end plate to $z = 1.65$ m.

In the LMD-U, the chamber length is 3.74 m. The total pump speed is 1000 liters/s. To achieve the same gas pressure as in the LMD, the number of injected particles is adjusted to $J_{inj} = 4.0 \times 10^{19}$ particle/s. As the standard case, the single pump is located at $z = 3.5$ m, but multiple pumps of 200, 200, 200, 400 L/s which are located at $z = 1.35$, 2.3, 2.9, 3.5 m, respectively, are also considered. The maximum magnitude of the magnetic field is 0.15 T.

Argon plasma with a radius of $a = 0.05$ m is considered. All plasma profiles are assumed to be axisymmetric and uniform in the axial direction. The electron n_e and the ion n_i densities are set to parabolic profiles

$$n_e(r) = n_i(r) = n_0\left(1 - \frac{r^2}{a^2}\right), \tag{3.1}$$

where $n_0 = 10^{19}\,1/\mathrm{m}^3$, while the electron and the ion temperatures are taken to be uniform in the radial direction for simplicity. The ion temperature is considered to be lower than 1 eV and it is set at $T_i = 0.5$ eV, while the electron temperature T_e changes from 3 eV up to 5 eV according to the experimental conditions. The temperature of the injected neutrals is set to 300 K (room temperature). The plasma generated in the production tube flows to the end plate in the main chamber. The plasma flow speed V_i is measured in terms of the Mach number $M = V_i/c_s$, where $c_s = \sqrt{2k_B T_e/M_i}$ is the reference speed, and M_i is the ion mass.

Since in low-energy range the self-elastic and ion collision cross sections are ambiguous, and since the results of the simulation are relatively insensitive to them, these

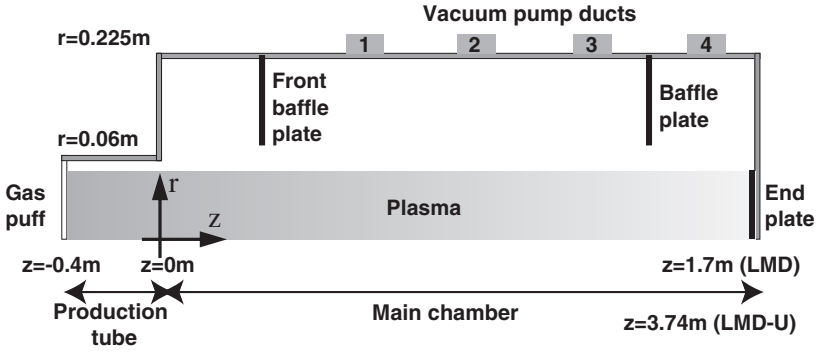

Fig. 2. Scheme of simulated devices. In the case of the LMD, only pump 4 is installed. The upgraded device supports multiple pumps (1–4) and a front baffle plate.

Table I. Parameters of LMD and LMD-U devices, single-pump case.

Device	Production tube		Main chamber		Vacuum pump (liter/s)	Gas puff (particle/s)	Magnetic field (T)
	diameter (m)	length (m)	diameter (m)	length (m)			
LMD	0.12	0.40	0.45	1.70	400	1.28×10^{19}	≤ 0.12
LMD-U	0.12	0.40	0.45	3.74	1000	4.00×10^{19}	≤ 0.15

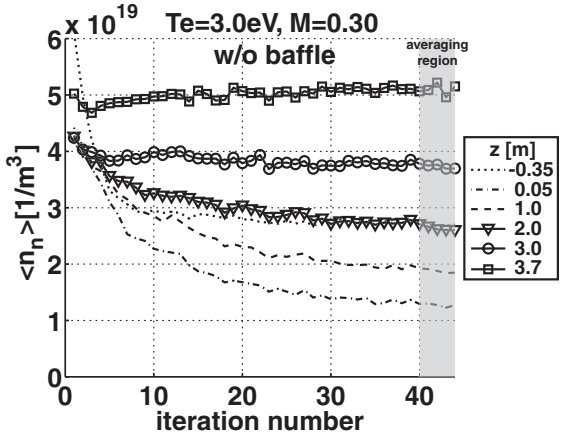

Fig. 3. Convergence of calculations at different positions within device (LMD-U: single pump, without baffle).

cross-sections are assumed to be constant: $\sigma_{\mathrm{els}} = 1.0 \times 10^{-18}\,\mathrm{m}^2$ and $\sigma_{\mathrm{mom}} + \sigma_{\mathrm{cxr}} = 4.0 \times 10^{-19}\,\mathrm{m}^2$. On the other hand, the neutral transport is very sensitive to the electron ionization in the expected electron temperature range. Thus, the following rate coefficient of analytic fitting is employed:[21)]

$$\langle \sigma_{\mathrm{ion}}(u)u \rangle = 2.34 \times 10^{-14} T_{\mathrm{e}}^{0.59} \mathrm{e}^{-17.44/T_{\mathrm{e}}}. \qquad (3.2)$$

Here, the unit of the rate coefficient is m^3/s and that of the electron temperature is eV.

Finally, the material surfaces of the device walls, end plate and baffle plates are assumed to be saturated by neutrals such that the reflection coefficient is unity. The calculation is typically performed using 30000 test particles for each source (gas injection at the production tube, recombination at the end plate of the main tube, and the recombination at the plasma surface).

3.2 Convergence

A fixed number of iterations is used to evaluate the neutral density profile, and in this subsection, the number of necessary iterations is discussed. The typical convergence of the radially averaged neutral density profile along the axial direction is shown in Fig. 3.

Within the first 20 iterations, the average profile changes strongly, particularly in the production tube and near the entrance of the main chamber. Then, the profile generally tends to converge to a final value, after typically 25 or 30 iterations. The required number of iterations depends on the parameters of the simulation. In the case of the LMD with the shorter main chamber length, the calculations converge faster and usually 20 iterations are used for the simulation. However, the required number of iteration can be more than 30 in the case of the LMD-U with a longer length. To guarantee the convergence, 40 iterations are typically used. In both cases, to reduce the statistical error, the results of the final 5 iterations are averaged.

3.3 Contribution of each source

In the present calculation, three neutral sources are taken into account, and these sources make different contributions to the total neutral profile. To see this, the neutral transport in a LMD-U is evaluated at two different electron temperatures. The results are shown in Fig. 4. In the simulation, the baffle plate is located at $z = 3.2\,\mathrm{m}$ and the Mach number is set to a relatively large value of $M = 0.4$.

In both cases, neutrals originating on the end plate or injected into the device are mainly localized near each source.

In the case of a low electron temperature ($T_{\mathrm{e}} = 3\,\mathrm{eV}$), the role of electron ionization is relatively small, and the neutral density in the main chamber is almost uniform in the radial direction. The profile increases toward the end plate due to the plasma flow [Figs. 4(a) and 4(b)]. The baffle plate and the junction of the plasma production tube and the main chamber cause the abrupt changes of neutral density profile seen in the axial profile. At each time moment, the pump system removes approximately 4% of neutrals, therefore it weakly affects the neutral density. The neutral density profile is mainly formed by recombination processes which produce about 96% of the neutral particles.

The effect of increasing the electron temperature is twofold: it enhances the electron ionization rate and it also increases the speed c_{s} (the plasma flow speed becomes faster even if the Mach number is constant). However, near the threshold energy of electron ionization, the plasma flow effect is weak in comparison with that of ionization, except for very large Mach numbers. Results for the electron temperature of $T_{\mathrm{e}} = 5\,\mathrm{eV}$ are shown in Figs. 4(c) and 4(d). In this case, the ionization MFP is less than the plasma diameter ($0.02 < \lambda_{\mathrm{ion}} < 0.10\,\mathrm{m}$). This results in the high recycling rate of neutrals, making this the dominant source of neutral particles. The neutral profile shows a steep radial gradient inside the plasma and it is almost uniform in the axial direction. As shown in the next subsection, the baffle plate obstructs the exhaust of these recycled neutrals, and the neutral pressure in the main chamber is higher than that in the vacuum pump region.

3.4 Effect of baffle plate

One of the possible tools used to control the neutral pressure in the main chamber is a baffle plate. It can prevent the free motion of neutrals and tends to localize the neutral pressure. In the following section, the dependence of the baffle-plate effect on some key parameters is studied.

First of all, the optimal axial position of the baffle plate is investigated (Fig. 5). To enhance the baffle-plate effect, the electron temperature is set to be low ($T_{\mathrm{e}} = 3\,\mathrm{eV}$) and the Mach numbers to be high [$M = 0.3$ (LMD) and $M = 0.4$ (LMD-U)]. Under such conditions, the plasma recombination rate is low and role of neutrals originating on the end plate is intensified.

The neutral density in the main chamber changes by inserting the baffle plate. However, the variation of the neutral density strongly depends on the position of the baffle plate, as shown in Figs. 5(a) and 5(b). The effect of the baffle plate becomes weaker as the baffle is located further away from the end plate. When the distance from the baffle plate to the end plate becomes larger, the number of ionized "end-plate particles" also becomes larger. Because of the steady state condition, these particles are recombinated in the plasma. Since in the present simulation, the plasma recombination rate is uniform in the axial direction,

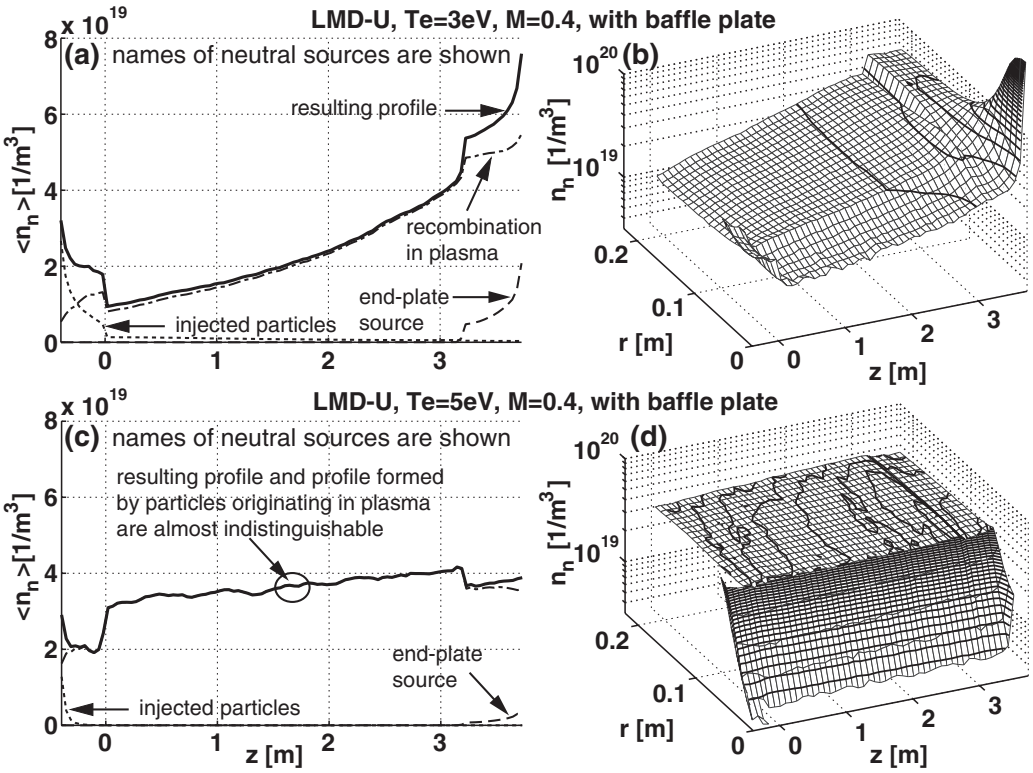

Fig. 4. (a,c) Contribution of each neutral source to resulting radially averaged profile and (b,d) corresponding two-dimensional view of resulting profile for LMD-U device with installed baffle and multiple pumps. In the case of $T_e = 5\,\mathrm{eV}$, the greatest contribution to the neutral density is from the plasma recombination source, such that lines indicating the injection and end-plate sources lie very close to zero and they are almost indistinguishable from the x-axis.

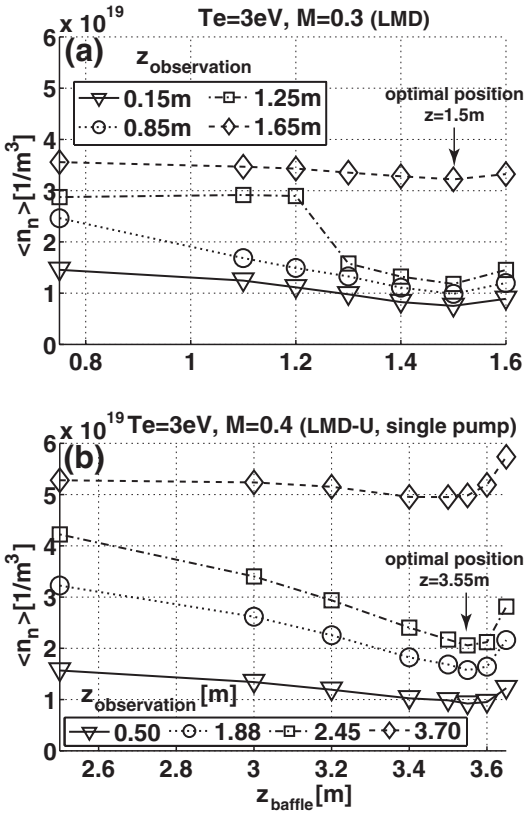

Fig. 5. Effect of baffle-plate position in (a) LMD and (b) LMD-U. In the LMD-U study, when $z_{\mathrm{baffle}} \geq 3.5\,\mathrm{m}$, the position of the pump duct is changed from $z = 3.5\,\mathrm{m}$ to $z = 3.7\,\mathrm{m}$.

recombinated particles weaken the baffle-plate effect. Note that the baffle effect also decreases when the baffle plate approaches the pump duct position. The reason is that the baffle reduces the volume of the region between the baffle plate and the end plate, and neutrals can easily escape to the main region [Fig. 5(a): $z_{\mathrm{baffle}} = 1.6\,\mathrm{m}$, and Fig. 5(b): $z_{\mathrm{baffle}} > 3.55\,\mathrm{m}$]. The optimal positions of the baffle in the LMD and LMD-U are found to be $z = 1.5$ and $3.55\,\mathrm{m}$, respectively. In the following calculations in the LMD-U, the baffle is set at $z_{\mathrm{baffle}} = 3.2\,\mathrm{m}$, the nearest available position to the end plate.[22] In both cases, the optimal distance from the end plate to the baffle is $0.2\,\mathrm{m}$.

In addition to the position, the baffle effect strongly depends on the plasma parameters. The number of neutral particles originating on the end plate is proportional to the speed of plasma flow. The increase in the Mach number correspondingly increases the neutral particle flux from the end plate, making the baffle-plate effect more pronounced. The electron temperature is also a key parameter. It affects the neutral density through changing the number of recycled particles and the speed of plasma flow. The increase in recycling weakens the baffle effect, while the high speed of plasma flow enhances it. Depending on the speed of plasma flow and the Mach number, the plate can increase or decrease the neutral density. The minimal Mach number, required so that the baffle decreases the neutral density is called the critical Mach number M_{crit}.

Figure 6 shows the dependence of the baffle-plate effect on the Mach number for the different electron temperatures in the LMD case. As a measure of the effect, the difference in neutral densities at the midpoint of the main chamber

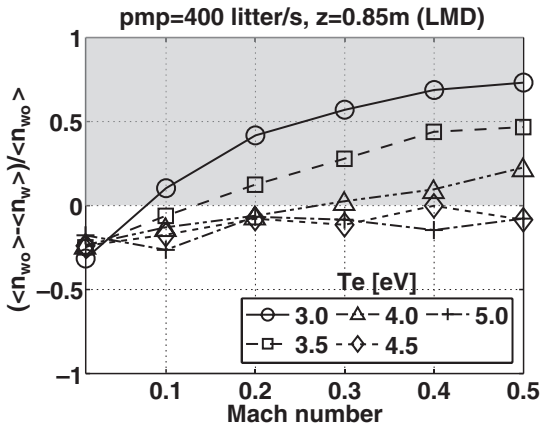

Fig. 6. Effect of Mach number on neutral density (LMD). The difference between the averaged neutral profile obtained with and without the baffle plate is shown. The gray region indicates the region where the baffle reduces the neutral density. The intersections of the lines with zero show the critical Mach number positions.

($z = 0.85$ m) with and without the baffle plate is plotted. The intersections of the lines with zero show the critical Mach number positions. It can be seen that, in the case of a low electron temperature, when recycling is weak, a small value of the Mach number $M_{\mathrm{crit}} \approx 0.08$ ($T_{\mathrm{e}} = 3$ eV) is sufficient to reduce the neutral density [$\langle n_{\mathrm{n}}(\mathrm{w/baffle})\rangle < \langle n_{\mathrm{n}}(\mathrm{w/o\ baffle})\rangle$]. At higher electron temperatures, the recycling of neutrals becomes important, and the corresponding critical Mach number also becomes higher: $M_{\mathrm{crit}} \approx 0.12$ ($T_{\mathrm{e}} = 3.5$ eV) and $M_{\mathrm{crit}} \approx 0.28$ ($T_{\mathrm{e}} = 4$ eV).

If $T_{\mathrm{e}} \geq 4.5$ eV, the critical Mach numbers become larger than 0.5, which are not shown in the figure. In this range of electron temperatures, the recycling of neutrals is the dominant source of neutrals, and the baffle plate prevents these recycled particles from moving to the vacuum pump region [$\langle n_{\mathrm{n}}(\mathrm{w/baffle})\rangle > \langle n_{\mathrm{n}}(\mathrm{w/o\ baffle})\rangle$ when $M < 0.5$]. In other words, the conductance to the vacuum pump region decreases as the electron temperature increases.

Results for the LMD-U are shown in Fig. 7. The neutral density is measured at $z = 1.875$ m (the midpoint of the main chamber). In the standard case with the single vacuum pump, the neutral density with the baffle plate is significantly higher than that without the baffle plate, even for the high Mach number of $M = 0.5$. In the larger LMD-U, recycling is more intensive than in the LMD. Since a large fraction of the recombinated particles originate at the plasma surface, the neutral density in the main tube is almost insensitive to the amount of neutrals originating on the end plate, that is, to the Mach number. In this case, the baffle plate prevents the movement of neutrals to the pump region and increases the neutral density in the main chamber. Another reason for the inefficiency of the baffle is that the baffle is located away from the optimal position.

A possible method of compensating or reducing the adverse effect of the baffle plate in the LMD-U is the use of a multiple-pump system. In Fig. 7(b), four vacuum pumps are set with sufficient spacing along the main chamber. The total pump capacity of 1000 L/s is the same as that in Fig. 7(a). In this case, three vacuum pumps, located in the main chamber, directly remove the recycled neutrals. The neutral density shows almost no dependence on the Mach

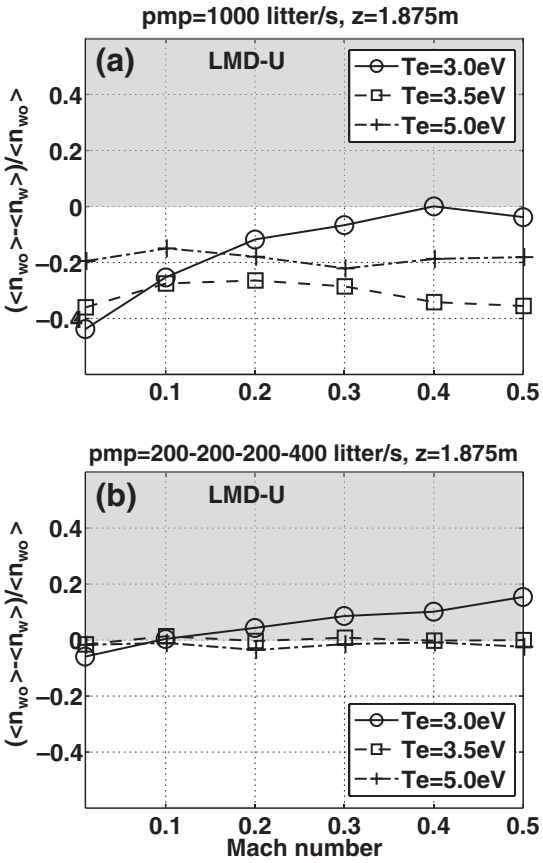

Fig. 7. Effect of Mach number on neutral density (a) LMD-U, single pump and (b) LMD-U, multiple pumps. The difference between the averaged neutral profile obtained with and without the baffle plate is shown.

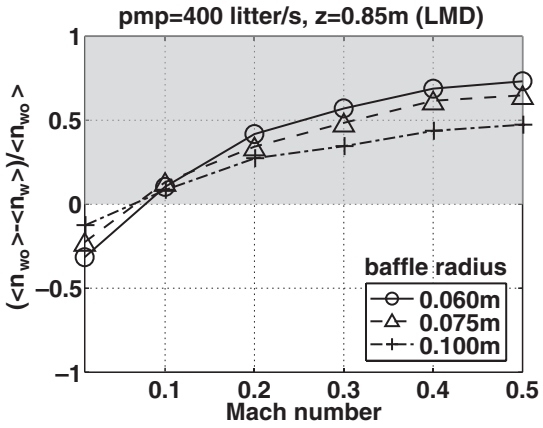

Fig. 8. Effect of baffle radius on neutral density (LMD). The difference between the averaged neutral profile obtained with and without the baffle plate is shown.

number, although a slight reduction of the density due to the baffle plate can be seen for $M > 0.1$ in the case of $T_{\mathrm{e}} = 3.0$ eV.

Finally, Fig. 8 shows the effect of the baffle radius on the neutral density for the LMD. Clearly, the increase in the baffle radius increases the conductance between the main chamber and the vacuum pump region and weakens the Mach number dependence. However, note that the critical Mach number does not change by changing the baffle radius.

3.5 *Effect of electron temperature*

As described above, the electron temperature is a key factor of the neutral transport. Since the electron ionization cross section strongly depends on the electron temperature, the temperature mainly affects the neutral transport through the electron ionization. When the ionization MFP is comparable to or longer than the plasma characteristic length, the recycling of neutrals is weak and the neutral density is almost uniform in the radial direction. Figure 9 shows the dependence of the neutral density inside the plasma ($r = 0.025$ m, $z = 1.875$ m) and the radially averaged density ($z = 0.875$ m) on the electron temperature in the case of the LMD-U with a multiple vacuum pump system. As expected, the neutral density inside the plasma sharply decreases from $n_n = (2-3) \times 10^{19}\,1/m^3$ ($T_e = 3.0$ eV) to $n_n \approx 5 \times 10^{18}\,1/m^3$ ($T_e = 5.0$ eV) with the increase in the electron temperature. The radially averaged neutral density increases with electron temperature and tends to saturate at some value. For this high recycling rate with a high electron temperature ($T_e \geq 4.0$) eV, the pump system removes less than 3% of the neutral particles and does not affect the neutral profile. At the same time, the high recycling rate and frequent self-collisions cause neutrals to fill the void region almost uniformly. Because of this uniformity, the saturation value of the neutral density is determined by the ratio of the injected neutral flux J_{inj} to the total pump speed [Fig. 9(b)].

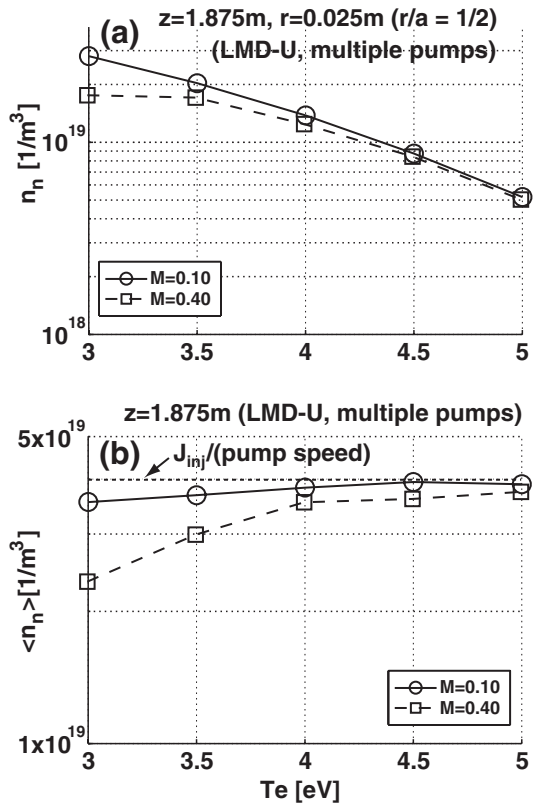

Fig. 9. (a) Effect of electron temperature on neutral density inside plasma at $r = 0.025$ m and (b) on averaged neutral profile LMD-U, with baffle plate).

3.6 *Effect of electron density*

Similar to the electron temperature, the plasma density also affects the neutral transport mainly through the electron ionization. In Fig. 10, the reference case is compared with the case of plasma density increased twofold (circles: reference cases, triangles: high density cases). If the recycling rate is high, the neutral density inside the plasma [Fig. 10(a)] can be roughly connected to that outside the plasma [Fig. 10(b)]. Indeed, since the ionization MFP is inversely proportional to the electron density and since the neutral density in the void region is hardly affected by the change in the electron density [as shown in Fig. 10(b)], a simple calculation gives the following estimation of the neutral density inside the plasma,

$$n_n(r) \approx [n_{n,ref}(r)]^{n_0/n_{0,ref}}, \tag{3.3}$$

where $n_0/n_{0,ref}$ is the ratio of the electron density in the studied case to the reference density.

In the present calculation, eq. (3.3) gives the neutral density of $n_n(r = 0.025\,\text{m}) \approx 7 \times 10^{17}\,1/m^3$ for $n_{n,ref}(r = 0.025\,\text{m}) \approx 5 \times 10^{18}\,1/m^3$ at $T_e = 5$ eV, while the simulation gives $n_n(r = 0.025\,\text{m}) \approx 1 \times 10^{18}\,1/m^3$.

3.7 *Effect of pumping speed*

In the LMD-U, it is possible to install a pump system with a total pump speed of 1400 L/s instead of 1000 L/s. The increase in the pump speed reduces the neutral density inversely proportionally to the pump speed, and this decrease in the neutral density is almost independent of other parameters such as electron temperature, as shown in Fig. 11 (crosses: the vacuum pump with the speed increased by a factor of 1.4).

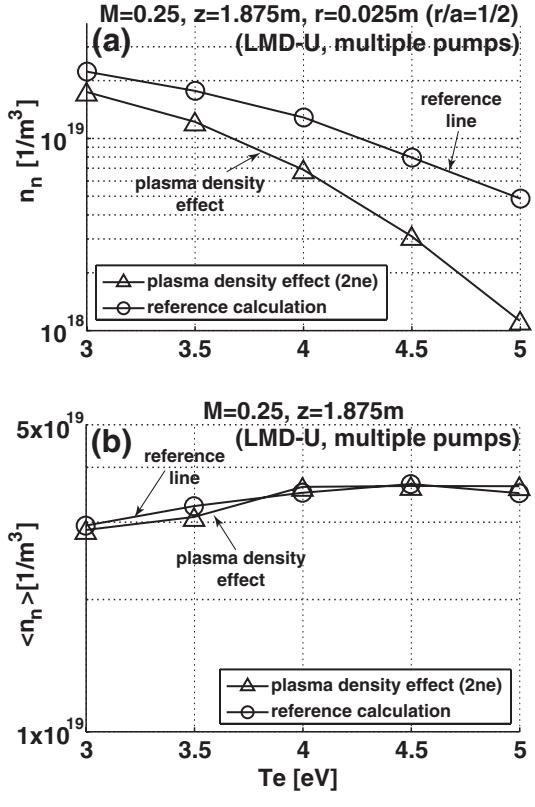

Fig. 10. (a) Effect of electron density on neutral density inside plasma at $r = 0.025$ m and (b) on averaged neutral profile (LMD-U, multiple pumps, without baffle plate). To demonstrate the effect, the neutral density was increased twofold in comparison with the reference case.

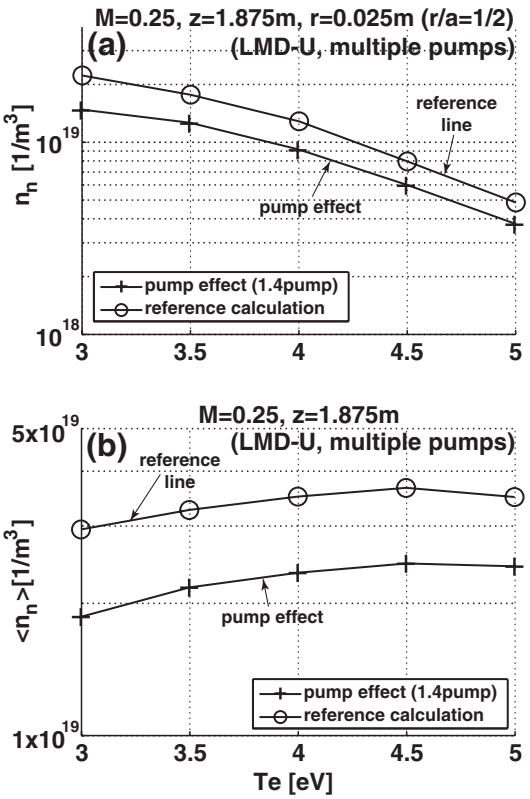

Fig. 11. (a) Effect of pumping speed on neutral density inside plasma at $r = 0.025$ m and (b) on averaged neutral profile (LMD-U, multiple pumps, without baffle plate). To demonstrate the effect, pumping speed was increased by factor of 1.4 in comparison with the reference case.

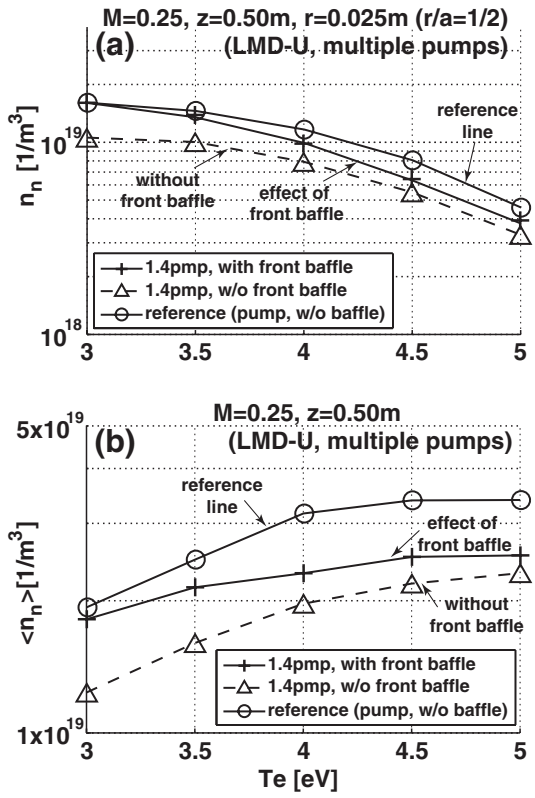

Fig. 12. (a) Effect of front baffle plate on neutral density inside plasma at $r = 0.025$ m and (b) on averaged neutral profile (LMD-U, multiple pumps, without rear baffle plate).

3.8 Effect of front baffle plate

Although the increase in the pump speed is effective for the reduction of the neutral density in the main chamber, it also decreases the neutral density in the production tube, which can affect the plasma production itself. A possible method of solving this this problem is to insert the front baffle plate near the junction of the production tube and the main chamber. In Fig. 12, the cases with a pump speed of 1.4 times faster with/without the front baffle plate inserted at $z = 0.75$ m are compared with the reference case (with standard pump speed and without any baffle plate). The Monte Carlo code does not take into account the effect of the plasma generation in the production region itself, and here the ability of the baffle to accumulate neutrals is simply demonstrated. The neutral densities, measured at $z = 0.50$ m between the junction and the front baffle plate, are plotted as a function of the electron temperature. Clearly, in the case of the higher pump speed without the front baffle plate, the neutral density is reduced by the same ratio of the pump speeds in the whole electron-temperature regime. However, in the case with the front baffle plate, the neutral density is almost the same as in the reference case for the lower electron temperature. In the higher electron-temperature case, the neutral density becomes lower in comparison with the reference value, since the high recycling rate tends to make the neutral density profile uniform in the axial direction. However, the reduction of the density is smaller than that in the case without a front baffle plate. These results show the possibility of using a front baffle plate to maintain a higher neutral density in and near the production tube.

4. Conclusions, Discussion, and Future Plans

4.1 Conclusions

A numerical model evaluating the neutral profile in the steady state based on the experimental parameters in a LMD and LMD-U was developed. The transport of neutral particles is calculated by the Monte Carlo technique, following the particle trajectory. Three neutral sources are considered: gas injection, the recombination of particles on the end plate, and the recombination in the plasma. The amount of plasma recombination source is determined on basis of the plasma parameters and the assumption of the steady-state condition.

The numerical scheme incorporates the main collision events. The electron impact ionization changes the number of neutral particles, and the ion–neutral collisions transfer the energy and momentum from the ions to the neutrals. The self-elastic collisions are also taken into account since they play an important role under the operational conditions. To handle the nonlinear self-elastic collision term, an iteration scheme is utilized.

Here, the effect of the plasma and the device parameters on the neutral transport is evaluated, on the basis of the experimental data and some assumptions. The main assumption made in the calculations is that the plasma density is uniform in the axial direction. In addition, the electron and ion temperatures are assumed to be uniform.

The numerical results show that the range of electron temperatures (from 3 up to 5 eV) assumed in experiments, can be divided into two parts.

At low electron temperatures (from 3 to 4 eV), the neutral level can be decreased by means of a baffle plate. The necessary conditions for a baffle plate to be effective are that (i) the distance from the baffle plate to the end plate (L_{bp-ep}) should be less than the ionization MFP, and (ii) the speed of the plasma flow should exceed a critical value M_{crit} depending on T_e and L_{bp-ep}. Otherwise, the baffle increases the neutral density in the main chamber. In the case of the LMD, $L_{bp-ep} = 0.2$ m, and the plate is effective in a plasma with T_e up to 4 eV. On the other hand, in the LMD-U with $L_{bp-ep} = 0.55$ m, the baffle plate is not effective even at $T_e = 3$ eV if a single pump is utilized. If multiple pumps are located separately along the main chamber, the baffle is efficient at the low electron temperature of $T_e = 3$ eV. In contrast, at higher electron temperatures, the recycling of neutrals diminishes the effect of the baffle plate. Another condition for the baffle plate to be effective is that the baffle radius should be as small as the plasma radius. Otherwise some of the particles originating at the end plate escape from the pump region, which reduces the baffle-plate efficiency. A similar effect occurs when the baffle plate is located too close to the end plate.

At higher electron temperatures (from 4 to 5 eV), where λ_{ion} is comparable to or less than the plasma diameter, the neutral density inside the plasma is considerably decreased by the electron impact ionization. On the other hand, outside the plasma, the neutral density is mainly determined by the neutral flux injected in the device and the speed of the pump system. The baffle plate is inefficient within this temperature range. In this sense, the neutral density in the core (which has drawback of inducing turbulence) is low. Thus, the weak influence of the baffle plate may be acceptable for studying turbulence.

The use of a faster pump system decreases the neutral density throughout the device, including the plasma production region. This may decrease the plasma production rate. To maintain the neutral density sufficiently high for efficient plasma production, the baffle plate can be inserted near the junction of the production tube and the main chamber. Similar to the rear baffle plate, this front baffle plate is only efficient at low electron temperatures.

As a conclusion, λ_{ion} is clarified to be a key parameter for controlling the neutral density and profile. It depends on a number of parameters, and their values should be considered together. For example, if the electron density is found to be twice the reference value, the baffle is inefficient when $T_e > 3.5$ eV instead of $T_e > 4$ eV.

4.2 *Discussion*

In the simulations presented in the paper, there are simplifications, validity of which should be verified in future studies.

First, for the sake of simplicity, the recombination in the plasma is assumed to be localized near the plasma surface to avoid the ambiguity of the source profile. Nevertheless the main properties of the profile still remain valid. This is supported by the following reason. The modeling of the recombination in the core is satisfactory in the limit where the plasma radius is much smaller than that of the chamber (as is in the present case). Thus, the present model is employed, and a quantitative elaboration should be prepared in future calculations.

The simulation shows that the baffle plate is not efficient for the case of the LMD-U. A more accurate physical model might change this conclusion. For example, one of the assumptions made is the uniform plasma density in the axial direction. The variation of the plasma parameters in that direction may affect the neutral transport and also the baffle-plate effect. Indeed, the electron density tends to decrease toward the end plate in experiments. This means that λ_{ion} is longer near the end plate, thus making the baffle plate more effective.

Another assumption, which can affect the neutral transport, is the uniform distribution of the plasma recombination source along the axial direction. This assumption holds when the ions move freely in the axial direction. In experiments, the ion temperature is low, and the ions are expected to have a finite flow velocity. Then, the recombination occurs close to the position of the ionization events or on the downstream side. Therefore, the neutral source tends to be localized at the high-recycling-rate region. This effect is expected to enhance the baffle-plate effect. The study of this effect requires more plausible plasma parameters in experiments and is a future study along with the effect of the nonuniformity of plasma parameters in the axial direction.

The results of simulation are also expected to be different when energy transport from ions to neutrals is taken into account. Since the ion–neutral collisions increase the temperature of the neutrals. Ionization MFP increases in length, enhancing the baffle plate efficiency.

4.3 *Future plans*

In future, an interface between the Monte Carlo and NLD codes will be developed. Similar to the Monte Carlo code, NLD uses experimental data as input parameters. Since direct measurements of the neutral profiles are difficult, the ion–neutral collision frequency, which depends on the neutral density, is assumed to be constant in the present simulations, where the frequency is an important parameter affecting the growth rate of the drift-wave instability. The incorporation of the Monte Carlo code into NLD allows us to improve the accuracy of calculations. The comparison of experimental data and the results of simulation will help us to understand the problem of turbulent structure formation.

Acknowledgment

This work is partly supported by a Grant-in-Aid for Specially Promoted Research from Ministry of Education, Culture, Sports, Science and Technology (16002005).

1) P. H. Diamond, S.-I. Itoh, K. Itoh, and T. S. Hahm: Plasma Phys. Control. Fusion **47** (2005) R35.
2) G. R. Tynan, R. A. Moyer, M. J. Burin, and C. Holland: Phys. Plasmas **8** (2001) 2691.
3) C. Schröder, O. Grulke, T. Klinger, and V. Naulin: Phys. Plasmas **12** (2005) 042103.
4) G. R. Tynan, C. Holland, J. H. Yu, A. James, D. Nishijima, M. Shimada, and N. Taheri: Plasma Phys. Control. Fusion **48** (2006) S51.
5) A. K. Sen, V. Sokolov, and X. Wei: Phys. Plasmas **13** (2006) 055905.
6) T. Kaneko, E. W. Reynolds, R. Hatakeyama, and M. E. Koepke: Phys.

Plasmas **12** (2005) 102106.
7) M. Koga and Y. Kawai: Phys. Plasmas **10** (2003) 650.
8) N. Kasuya, M. Yagi, and K. Itoh: J. Plasma Phys. **72** (2006) 957.
9) S. Shinohara, Y. Miyauchi, and Y. Kawai: Plasma Phys. Control. Fusion **37** (1995) 1015.
10) S. Shinohara, T. Nishijima, M. Kawaguchi, K. Terasaka, Y. Nagashima, Y. Kawai, A. Fujisawa, M. Yagi, K. Itoh, and S.-I. Itoh: presented at Spring Meet. Physical Society of Japan, 2006 [in Japanese].
11) Y. Saitou, A. Yonesu, S. Shinohara, M. V. Ignatenko, N. Kasuya, M. Kawaguchi, K. Terasaka, T. Nishijima, Y. Nagashima, K. Kawai, M. Yagi, S.-I. Itoh, M. Azumi, and K. Itoh: submitted to Phys. Plasmas.
12) N. Kasuya, M. Yagi, M. Azumi, K. Itoh, and S.-I. Itoh: to be published in J. Phys. Soc. Jpn.
13) J. W. Connor: Plasma Phys. **19** (1977) 853.
14) M. A. Lieberman and A. J. Lichtenberg: *Principles of plasma discharges and material processing* (Wiley, New Jersey, 2005) 2nd ed., p. 727.
15) D. Heifetz: in *Physics of Plasma–Wall Interactions in Controlled Fusion*, ed. D. E. Post and R. Behrisch (Plenum, New York, 1986) p. 695.
16) J. M. Hammersley and D. C. Handscomb: *Monte Carlo Methods* (Wiley, New York, 1964).
17) E. E. Lewis and W. F. Miller: *Computational Methods of Neutron Transport* (Wiley, New York, 1984) p. 296.
18) M. H. Hughes and D. E. Post: J. Comput. Phys. **28** (1978) 43.
19) D. Heifetz, D. Post, M. Petravic, J. Weisheit, and G. Bateman: J. Comput. Phys. **46** (1982) 309.
20) G. J. M. Hagelaar, F. J. de Hoog, and G. M. W. Kroesen: Phys. Rev. E **62** (2000) 1452.
21) J. T. Gudmundsson: Univ. Iceland Tech. Rep. RH-21-2002 (2002).
22) The space close to the end plate is occupied by the pump duct. To find the optimal position of the baffle, the pump position is shifted from $z = 3.2$ to 3.7 m when $z_{\mathrm{baffle}} \geq 3.5$ m.